

**Keywords:** endometrial carcinoma; histomorphological marker; dynamic contrast-enhanced magnetic resonance imaging (DCE-MRI); diffusion-weighted imaging (DWI); biomarker; angiogenesis

# Increased microvascular proliferation is negatively correlated to tumour blood flow and is associated with unfavourable outcome in endometrial carcinomas

I S Haldorsen<sup>\*1,2</sup>, I Stefansson<sup>3,4</sup>, R Grüner<sup>1,5</sup>, J A Husby<sup>1,2</sup>, I J Magnussen<sup>1</sup>, H M J Werner<sup>6,7</sup>, Ø O Salvesen<sup>8</sup>, L Bjørge<sup>6,7</sup>, J Trovik<sup>6,7</sup>, T Taxt<sup>1,9</sup>, L A Akslen<sup>3,4</sup> and H B Salvesen<sup>6,7</sup>

<sup>1</sup>Department of Radiology, Haukeland University Hospital, Jonas Liesvei 65, Postbox 7800, 5021 Bergen, Norway; <sup>2</sup>Section for Radiology, Centre for Cancer Biomarkers, Department of Clinical Medicine, University of Bergen, 5020 Bergen, Norway; <sup>3</sup>Centre for Cancer Biomarkers, The Gade Institute, Department of Clinical Medicine, University of Bergen, 5020 Bergen, Norway; <sup>4</sup>Department of Pathology, Haukeland University Hospital, 5021 Bergen, Norway; <sup>5</sup>Department of Physics and Technology, University of Bergen, 5020 Bergen, Norway; <sup>6</sup>Department of Obstetrics and Gynaecology, Haukeland University Hospital, 5021 Bergen, Norway; <sup>7</sup>Centre for Cancer Biomarkers, Department of Clinical Science, University of Bergen, 5020 Bergen, Norway; <sup>8</sup>Unit for applied Clinical Research, Department of Cancer Research and Molecular Medicine, Norwegian University of Science and Technology, Postbox 8905, 7491 Trondheim, Norway and <sup>9</sup>Department of Biomedicine, University of Bergen, 5020 Bergen, Norway

**Background:** We aimed to study the angiogenic profile based on histomorphological markers in endometrial carcinomas in relation to imaging parameters obtained from preoperative dynamic contrast-enhanced magnetic resonance imaging (DCE-MRI) and diffusion-weighted imaging (DWI) and to explore the potential value of these markers to identify patients with poor outcome.

**Methods:** In fifty-four surgically staged endometrial carcinoma patients, immunohistochemical staining with factor VIII and Ki67 allowed assessment of microvessel density (MVD) and microvascular proliferation reflecting tumour angiogenesis. In the same patients, preoperative pelvic DCE-MRI and DWI allowed the calculation of parameters describing tumour microvasculature and microstructure *in vivo*.

**Results:** Microvascular proliferation was negatively correlated to tumour blood flow (Fb) ( $r = -0.36$ ,  $P = 0.008$ ), capillary permeability surface area product (PS) ( $r = -0.39$ ,  $P = 0.004$ ) and transfer from the blood to extravascular extracellular space (EES) (Ktrans) ( $r = -0.40$ ,  $P = 0.003$ ), and was positively correlated to tumour volume ( $r = 0.34$ ;  $P = 0.004$ ). High-tumour microvascular proliferation, low Fb and low Ktrans were all significantly associated with reduced progression/recurrence-free survival ( $P < 0.05$ ).

**Conclusion:** Disorganised angiogenesis with coexisting microvascular proliferation and low tumour blood flow is a poor prognostic factor supporting that hypoxia is associated with progression and metastatic spread in endometrial carcinomas.

Endometrial cancer is the most common pelvic gynaecologic malignancy in industrialised countries, and the incidence is increasing (Amant *et al*, 2005). Treatment and prognosis are

influenced by the surgical International Federation of Gynaecology and Obstetrics (FIGO) staging system and by histological subtype and grade (Amant *et al*, 2005; Pecorelli, 2009). Although ~75% of

\*Correspondence: Professor IS Haldorsen; E-mail: [ingfrid.haldorsen@helse-bergen.no](mailto:ingfrid.haldorsen@helse-bergen.no)

Revised 27 August 2013; accepted 10 October 2013; published online 31 October 2013

© 2014 Cancer Research UK. All rights reserved 0007–0920/14

the patients have tumours confined to the uterine corpus at the time of primary diagnosis, suggesting a favourable prognosis, 15–20% of these tumours recur with an aggressive and therapy-resistant behaviour (Salvesen *et al*, 2012).

Angiogenesis is essential for tumour growth, invasion and metastatic spread. Tumour-associated vessels are structurally and functionally abnormal, typically exhibiting increased permeability, delayed maturation and potential for rapid proliferation (Fox *et al*, 2001; Baluk *et al*, 2003). For endometrial carcinomas, histological biomarkers reflecting the angiogenic phenotype of the tumour, such as microvascular density (MVD) and vascular proliferation have been identified as prognostic markers (Stefansson *et al*, 2006).

Dynamic contrast-enhanced magnetic resonance imaging (DCE-MRI) is a novel functional imaging technique that allows a quantitative assessment of tissue perfusion and vascular permeability. This imaging technique enables characterisation of tumour microvasculature and depiction of the angiogenic profile *in vivo* (Tofts *et al*, 1999; Leach *et al*, 2012). Diffusion-weighted imaging (DWI) is another functional MRI technique that characterises tissue microstructure based on water-diffusion properties, which are considered surrogate markers of tumour cellularity and cellular membrane integrity (Padhani *et al*, 2009). Both functional imaging methods, when performed as an adjunct to routinely applied conventional MRI (Amant *et al*, 2005; Haldorsen and Salvesen, 2012), may provide preoperative functional tumour characterisation with potential relevance for clinical phenotype and preoperative risk stratification in endometrial carcinoma patients.

This study explores the angiogenic profile of tumours based on histomorphological markers in relation to perfusion/permeability and diffusion parameters obtained from preoperative functional MRI in endometrial carcinoma patients. The value of the histomorphological markers and of functional MRI parameters in reflecting clinical phenotype, and in identification of patients with poor outcome in primary endometrial carcinomas, is also explored.

## MATERIALS AND METHODS

**Patient series, study setting and clinical outcome.** This prospective study was conducted under institutional review board-approved protocols with informed consent from all patients. From May 2009 to February 2011 preoperative pelvic MRI, which included DCE-MRI and DWI was performed in 55 patients in whom the diagnosis of endometrial carcinoma was subsequently histologically verified at surgical staging. In 54 (out of 55) patients, sufficient tumour tissue was available to allow staining with immunohistochemical markers, and these patients constituted the study sample ( $n = 54$ ). All patients were diagnosed and treated at the same university hospital, which is a European Society for Gynaecologic Oncology accredited cancer centre serving a population of ~1 million inhabitants.

Follow-up data regarding recurrence, progression and survival have been collected from patient records and from correspondence with the responsible primary physicians or gynaecologists. Date of last follow-up was February 2013 and mean follow-up for survivors was 23 months (range 6–40).

**Histological diagnosis and immunohistochemistry.** All patients were surgically staged according to the revised FIGO staging system (2009) (Pecorelli, 2009). Surgical specimens were sectioned along the longitudinal plane of the uterus, and myometrial invasion and cervical stromal invasion were estimated grossly and confirmed microscopically according to standard procedures (Silverberg *et al*, 2003). Routine histopathology reports were generated without the knowledge of preoperative MRI findings.

The pathologists documented the numbers and size of metastatic lymph nodes.

Immunohistochemical staining was performed with factor VIII and Ki67 enabling calculation of three parameters:

**Microvessel density.** The average number of microvessels within selected tumour areas was estimated. Sections were first examined at low magnifications ( $\times 25$ ,  $\times 100$ ) to identify the most vascular areas of the tumours (i.e., areas with most intense factor VIII staining and the apparently highest density of microvessels) (Weidner *et al*, 1991). Subsequently, 10 fields ( $\times 250$ ; field size,  $0.424 \text{ mm}^2$ ) were examined, except in a few cases in which less tumour tissue was available. The counts were expressed as the average of all fields examined ( $\text{MVD}_{\text{mean}}$ ; vessels per  $\text{mm}^2$ ).

**Microvascular proliferation.** Proliferating endothelial cells were recognised by their morphology, localisation and distinct Ki-67/factor VIII co-expression. Positive nuclei outside the endothelial cell layer, or within the vessel lumen, were avoided. Microvascular proliferation was expressed as average number of proliferation microvessels with Ki-67-positive endothelial cells of all fields examined (proliferating vessels per  $\text{mm}^2$ ).

**Vascular proliferation index.** Vascular proliferation index (VPI) is expressed by the ratio between the number of proliferating microvessels with Ki-67-positive endothelial cells (regardless of the number of positive endothelial cells per vessel) and the total number of factor VIII-positive microvessels (%), as examined within selected hotspot areas.

**Magnetic resonance imaging protocol.** Magnetic resonance imaging was performed on a 1.5T Siemens Avanto running Syngo MR B17 (Erlangen, Germany) using a six-channel body coil. Before imaging, 20 mg butylscopolamine bromide (Buscopan, Boehringer Ingelheim, Germany) was administered intravenously. The protocol included standard diagnostic MR imaging based on Guidelines of the European Society of Urogenital Imaging and functional imaging (Kinkel *et al*, 2009), which included DCE-MRI and DWI. Mean (range) interval between MR examination and surgical staging was 8.1 (1–36) days.

**Structural MRI.** This included pelvic sagittal and axial oblique (perpendicular to the long axis of the uterus) T2-weighted images and axial oblique T1-weighted gradient-echo images obtained before and after intravenous contrast administration (Dotarem, Guerbet:  $0.1 \text{ mmol}$  gadolinium per kilogram of body weight,  $3 \text{ ml s}^{-1}$  injection speed) using 2-min delay (Haldorsen *et al*, 2012). In addition, abdominal axial T1-weighted images and axial and coronal T2-weighted images were acquired up to the renal hila to assess lumboaortic lymphadenopathy.

**Physiological MRI.** Pelvic DCE-MRI was acquired with 12 axial slices using a 3D spoiled gradient echo (FLASH) sequence (echo time/repetition time (TE/TR) =  $1.05/2.64 \text{ ms}$ , flip angle (FA) =  $12^\circ$ , matrix =  $256 \times 256$ , field of view (FOV) =  $30 \times 30 \text{ mm}^2$ , slice thickness =  $5 \text{ mm}$ , number of averages (NA) = 1) with a temporal resolution of  $2.49 \text{ s}$  (Haldorsen *et al*, 2013). Sequential images were obtained from 30 s before administration of i.v. contrast to 6.3 min after i.v. contrast, with a pause of 33 s at 2 min post contrast (in order to acquire the diagnostic T1-weighted contrast-enhanced series). Multiple precontrast images were also acquired with different FAs of 4, 8, 12 and  $15^\circ$ .

Pelvic DWI was acquired using an axial 2D echo planar imaging (EPI) sequence with b-values of 0 and  $1000 \text{ s mm}^{-2}$  (TE/TR =  $79/3100 \text{ ms}$ , matrix =  $128 \times 128$ , FOV =  $30 \times 30 \text{ mm}^2$ , slice thickness =  $5 \text{ mm}$ , NA = 12).

**Data analysis.** All images were analysed using NordicICE v.2.3.12 (NordicNeuroLab Inc., Bergen, Norway) by a radiologist (ISH with >7 years of experience with pelvic MR imaging) who was blinded for tumour stage, histological diagnosis and patient outcome. Standard images were used in combination with the physiological images for verification of anatomical structures and tumour location. Regions of interest (ROIs) were subsequently drawn manually on one functional image 2 min post contrast in each patient. Regions of interest were drawn directly on the functional images to avoid registration artefacts between structural and physiological images.

Two circular ROIs were drawn on the DCE-MRI series on the same single slice for each patient: ROI no. 1 was placed within the tumour avoiding necrotic or haemorrhagic areas and ROI no. 2 in a pelvic artery. The volume of ROI no. 1 had a median of 0.25 ml (mean 0.32 ml; range, 0.05–0.96 ml) and varied due to variable tumour size. The quality of the vessel signals in ROI no. 2 differed substantially between patients, most likely due to turbulence or flow artefacts. Thus, a population-based vessel signal, which was individually optimised in each patient using a blind source separation technique (Gruner and Tact, 2006; Tact *et al.*, 2012), was used.

Because of the high temporal resolution in the dynamic series (~2.5 s), a two-compartment model incorporating both capillary flow and permeability was chosen. An in-house implementation of the adiabatic approximation model of Johnson and Wilson (aaJW) (St Lawrence and Lee, 1998; Tact *et al.*, 2012) was thus used to analyse the contrast concentration curves in the myometrium and tumour regions in each patient. The time courses in each ROI were independently interpolated using a cubic spline interpolation (Matlab v.7.7, Mathworks Inc., Natick, MA, USA) to compensate for the time gap when the high-resolution T1-weighted images were acquired. Multiple precontrast flip angle acquisitions were used to convert from MR signal-intensities to contrast agent concentrations in time (Tact *et al.*, 2012). No temporal filtering or other smoothing was applied to the data. This model allowed the calculation of four independent parameters describing the tissue microvasculature: blood flow (Fb), extraction fraction (E), intravascular/capillary transit time (Tc) and transfer constant from extravascular extracellular space (EES) to the blood (Kep); and four derived parameters: blood volume (Vb) ( $Vb = Fb \times Tc$ ), volume of EES (Ve) ( $Ve = (E \times Fb)/Kep$ ), capillary permeability surface area product (PS) ( $E = 1 - \exp(-PS/Fb(1 - rHematocrit))$ ) and transfer from the blood to EES (Ktrans) ( $Ktrans = E \times Fb$ ) (Tact *et al.*, 2012). Additionally, the integrated area under the concentration time curve (IAUGC) over 60 and 180 s was calculated to allow a non-model-based quantitative assessment of tumour enhancement (Leach *et al.*, 2012).

Values for ADC were measured in ROIs of tumour tissue on the ADC map. Tumour volume was estimated based on the standard anatomical images with measurements of maximum tumour diameter in three orthogonal planes (x, y and z) using the following equation: Tumour volume =  $x \times y \times z/2$ .

**Statistical analysis.** The non-parametric Kolmogorov-Smirnov test for normality was used to verify the normality assumption for the continuous variables analysed. The correlation between continuous variables (imaging parameters and angiogenic markers) was evaluated using the Pearson bivariate correlation test.

Median values were applied to explore the prognostic value of categories for the imaging parameters and angiogenic markers. Univariate analyses of time to recurrence (for patients considered cured by primary treatment) or progression (for patients known to have residual disease after primary treatment) were performed using the Kaplan–Meier test. Differences in recurrence-/progression-free survival were assessed by the Mantel–Cox (log rank) linear trend test. The Cox proportional hazards model was used to

study the effect on survival of continuous variables. The data were analysed using SPSS v. 20.0 (Chicago, IL, USA). All reported *P*-values were two-sided and considered to indicate statistical significance when less than 0.05.

## RESULTS

**Patients.** Clinicopathological characteristics are listed in Table 1. All patients were primarily treated with bilateral salpingo-oophorectomy and hysterectomy consisting of simple hysterectomy in 94% (51/54) and radical hysterectomy in 6% (3/54). Pelvic lymph node sampling was performed in 89% (48/54) as part of the routine surgical staging procedure. In 33% (18/54) of the patients adjuvant therapy was given: 24% (13/55) had chemotherapy and 9% (5/54) had external pelvic radiation.

Median tumour size assessed by structural MRI was 5.9 ml (mean, 31.9; range, 0.1–611.0).

**Angiogenic markers based on immunohistochemistry.** Median microvessel density (MVD) was 47 (mean, 49; range, 15–97) microvessels per mm<sup>2</sup>. Median microvascular proliferation was 7 (mean, 7.6; range, 0–21) vessels/mm<sup>2</sup>, whereas median VPI was 3.0% (mean, 4.1%; range, 0–13.6%).

**Physiological tumour parameters based on MRI.** On the basis of DCE-MRI the independent physiological parameters reflecting microvasculature in the tumour tissue had a median of 9.3 (mean, 9.6; range 2.2–17.8) ml per 100 ml min<sup>-1</sup> for blood flow (Fb); 0.39% (mean, 0.39%; range 0.24–0.67%) for extraction fraction (E); 14.9 (mean, 15.0; range, 7.5–27.4) seconds for intravascular capillary transit time (Tc); and 0.29 (mean, 0.30; range, 0.10–0.55) per min for the transfer constant from EES to blood (Kep). The derived parameters had a median of 1.9 (mean, 2.2; range, 0.5–5.2) ml per 100 ml for blood volume (Vb); 11.9 (mean, 12.6; range, 3.9–29.4) ml per 100 ml for fractional volume

Table 1. Clinicopathological patient characteristics

Clinicopathological characteristics	n = 54
Age; mean (range) years	67 (41–93)
Postmenopausal, n (%)	48 (89)
<b>Histological subtype, n (%)</b>	
Endometrioid	42 (78)
Clear cell	2 (4)
Serous papillary	6 (11)
Carcinosarcoma	3 (6)
Undifferentiated	1 (2)
<b>Tumour grade, n (%)</b>	
Grade 1	17 (32)
Grade 2	11 (20)
Grade 3	26 (48)
<b>FIGO stage<sup>a</sup>, n (%)</b>	
1A	23 (43)
1B	14 (26)
2	6 (11)
3B	1 (2)
3C1	4 (7)
3C2	5 (9)
4B	1 (2)
Abbreviation: FIGO = International Federation of Gynaecology and Obstetrics.	
<sup>a</sup> According to FIGO 2009 staging criteria (Pecorelli, 2009).	

of EES (Ve); 3.3 (mean, 3.4; range, 0.8–7.0) ml per 100 ml min<sup>−1</sup> for capillary permeability surface area product (PS); and 2.6 (mean, 2.6; range, 0.6–5.2) ml per 100 ml min<sup>−1</sup> for transfer from the blood to EES (Ktrans). Integrated area under the concentration time curve in the tumour had a median of 0.51 (mean, 0.57; range, 0.40–1.07) mms over 60 s and a median of 2.71 (mean, 2.87; range, 1.67–5.02) mms over 180 s.

Median ADC value in endometrial carcinoma tissue was 0.78 (mean, 0.82; range 0.60–1.20)x10<sup>−3</sup> mm<sup>2</sup> s<sup>−1</sup>.

**Correlation between angiogenic markers and imaging parameters.** Microvascular proliferation was negatively correlated to tumour blood flow (Fb) ( $r = -0.36$ ,  $P = 0.008$ ) (Figure 1A) and IAUGC over 60 s ( $r = -0.28$ ,  $P = 0.04$ ) and 180 s ( $r = -0.36$ ,  $P = 0.007$ ) (Table 2). Microvascular proliferation was also negatively correlated to capillary permeability surface area product

(PS) ( $r = -0.39$ ,  $P = 0.004$ ) and transfer from blood to EES (Ktrans) ( $r = -0.40$ ,  $P = 0.003$ ), and was positively correlated to tumour volume ( $r = 0.34$ ;  $P = 0.004$ ) (Figure 1B) (Table 2). Similar but less significant correlations were observed between vascular proliferation index and tumour capillary permeability surface area product (PS) and transfer from blood to EES (Ktrans) ( $P = 0.04$  for both).

No significant correlations were observed between the other physiological imaging parameters and the angiogenic markers; however, there were tendencies to positive correlation between microvascular proliferation and capillary transit time (Tc) ( $r = 0.24$ ,  $P = 0.09$ ) and negative correlations with the transfer constant from EES to blood (Kep) ( $r = -0.22$ ,  $P = 0.10$ ), blood volume (Vb) ( $r = -0.23$ ,  $P = 0.09$ ) and fractional volume of EES (Ve) ( $r = -0.26$ ,  $P = 0.06$ ).

**Prognostic value of angiogenic markers and imaging parameters.** When ranked into two categories (using median limits) high microvascular proliferation (Figure 2A), high vascular proliferation index and high MVD were all significantly associated with reduced progression/recurrence-free survival ( $P < 0.05$ ) in endometrial carcinomas (Figures 3 and 4). Low tumour blood flow (Fb) (Figure 2B), low transfer from the blood to EES (Ktrans) and high capillary transit time (Tc) were also associated with reduced progression/recurrence-free survival ( $P < 0.05$ ).

When analysing the parameters as continuous variables, blood flow (Fb) and capillary transit time (Tc) had a significant impact on recurrence/progression-free survival with univariate hazard ratios of 0.77 (95% CI, 0.61–0.97;  $P = 0.03$ ) and 1.17 (95% CI, 1.03–1.32;  $P = 0.02$ ), respectively.

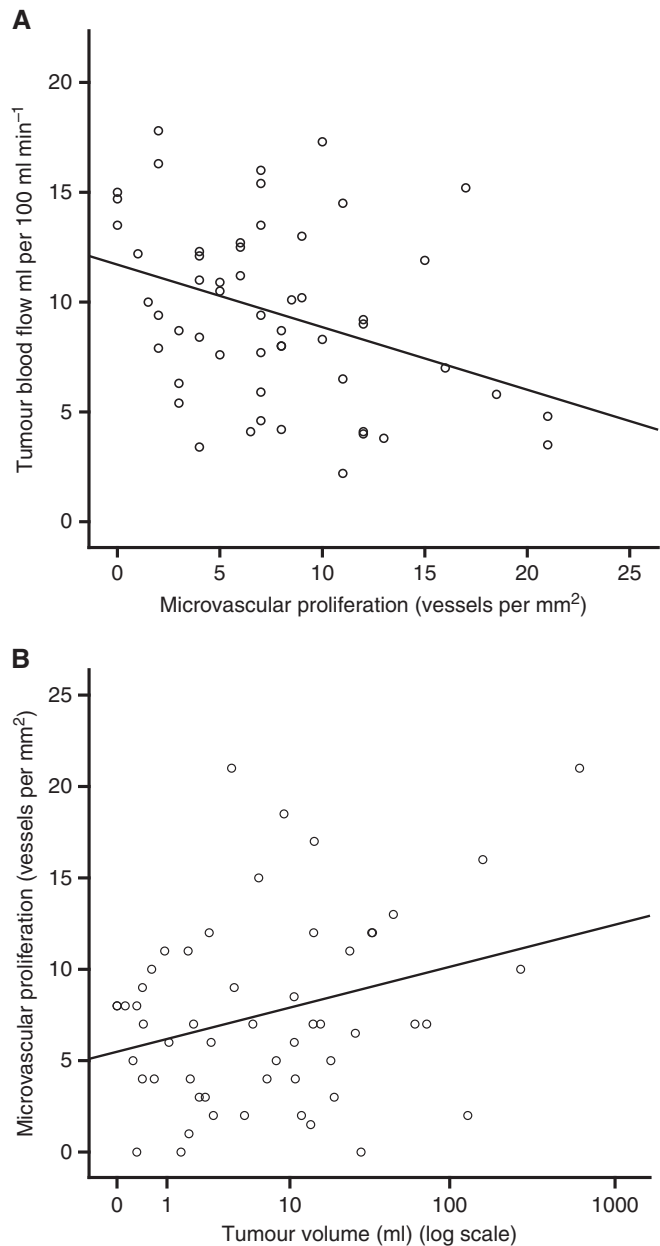


**Figure 1.** Scatterplots depicting the negative correlation between microvascular proliferation in tumour tissue and estimated tumour blood flow ( $r = -0.359$ ,  $P = 0.008$ ;  $n = 54$ ) (A) and the positive correlation between microvascular proliferation in tumour tissue and tumour volume (log scale) ( $r = 0.338$ ,  $P = 0.004$ ;  $n = 54$ ) (B).

Table 2. Correlation between angiogenesis markers by immunohistochemistry and imaging markers in tumour tissue-based on preoperative DCE-MRI (perfusion markers), DWI (diffusion marker) and conventional MRI (tumour volume) in endometrial carcinomas (n = 54)		
Imaging markers	Microvessel density <i>r</i> <sup>a</sup> ( <i>P</i> <sup>b</sup> )	Microvascular proliferation <i>r</i> <sup>a</sup> ( <i>P</i> <sup>b</sup> )
Perfusion		
Fb; blood flow	− 0.03 (0.83)	− <b>0.36 (0.008)</b>
Tc; capillary transit time	0.04 (0.79)	0.24 (0.09)
E; extraction fraction	− 0.03 (0.82)	0.00 (0.97)
Kep; transfer constant from EES to blood	0.15 (0.26)	− 0.22 (0.10)
Vb; blood volume	0.01 (0.97)	− 0.23 (0.09)
Ve; fractional volume of EES	− 0.10 (0.49)	− 0.26 (0.06)
PS; capillary permeability surface area product	− 0.04 (0.79)	− <b>0.39 (0.004)</b>
Ktrans; transfer from blood to EES	− 0.03 (0.84)	− <b>0.40 (0.003)</b>
IAUGC over 60 s	− 0.21 (0.12)	− <b>0.28 (0.04)</b>
IAUGC over 180 s	− 0.15 (0.27)	− <b>0.36 (0.007)</b>
Diffusion		
ADC value	0.12 (0.38)	0.06 (0.65)
Anatomical imaging		
Volume	− 0.12 (0.39)	<b>0.34 (0.004)</b>
Abbreviations: ADC = apparent diffusion coefficient; IAUGC = integrated area under the concentration time curve; DCE-MRI = dynamic contrast-enhanced magnetic resonance imaging; DWI = diffusion-weighted imaging; EES = extravascular extracellular space. Significant correlations are shown in bold. Independent imaging parameters are listed in italic.		
<sup>a</sup> Pearson correlation coefficient.		
<sup>b</sup> Pearson bivariate correlation test.		



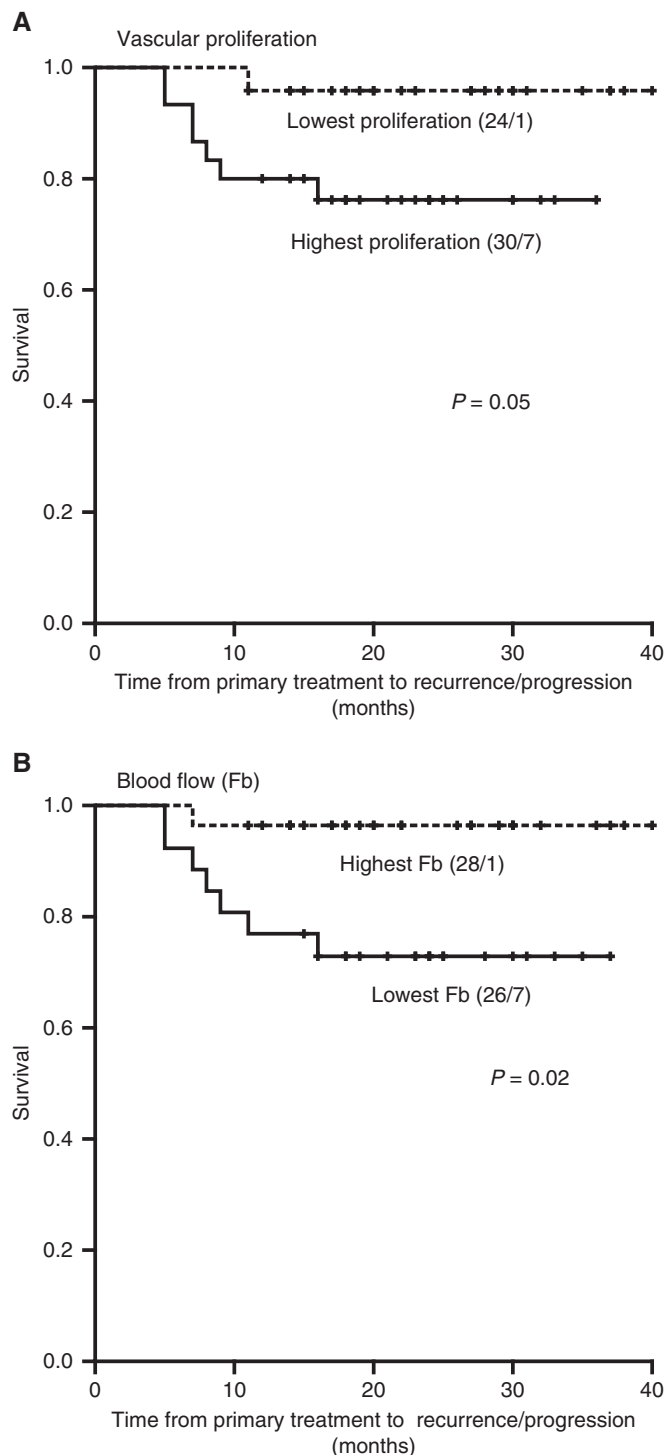


Figure 2. Kaplan-Meier curves depicting recurrence/progression-free survival according to microvascular proliferation (**A**) and tumour blood flow (Fb) (**B**). For each category: number of cases/number of cases with recurrence or progression.  $P$ -values refer to the Log Rank test.

## DISCUSSION

This is, to our knowledge, the first study comparing measures of tumour vasculature *in vivo* based on quantitative DCE-MRI with measures of intra-tumour angiogenesis in tumour samples in endometrial carcinoma patients. Interestingly, we found that prognostic immunohistochemical markers reflecting microvascular

proliferation were significantly correlated to markers of tumour tissue perfusion and permeability obtained from DCE-MRI measurements. Furthermore, these DCE-MRI markers also predicted recurrence/progression-free survival. Thus, we assume that the increased microvascular proliferation in endometrial carcinoma tissue detected has its correlate in specific alterations of the functional status of the tumour vasculature *in vivo*, with potential relevance for tumour progression and metastatic spread.

The two-compartment model applied for calculation of the parameters describing the microvasculature has some inherent inaccuracies and pitfalls. The use of a population-based arterial input function may confound the results when the cardiac output or the vascular resistance differ between patients (Leach *et al*, 2012). Furthermore, the two-compartment model assumes blood flow not to be a rate-limiting step; if incorrect, the assessment of the derived parameters are potentially flawed, and should thus be interpreted with care. The validity the DCE-MRI parameter Fb in this study is, however, supported by the finding that estimated blood flow (Fb) significantly correlated to the non-model-based parameter IAUGC over 180 s ( $r = 0.53$ ,  $P < 0.001$ ).

Negative correlations between microvascular proliferation and the DCE-MRI parameter blood flow (Fb) as well as the non-model-based parameters IAUGC over 60 s and 180 s (Table 2) were observed, indicating that reduced blood flow is a hallmark of tumours exhibiting increased microvascular proliferation. Furthermore, microvascular proliferation also negatively correlated with capillary permeability surface area product (PS) and transfer from the blood to EES (Ktrans), both parameters being derived from the blood flow (Fb) and from the extraction fraction (E) reflecting capillary leakage; thus PS and Ktrans reflect characteristics of both tumour perfusion and capillary permeability. Although no correlation was observed between microvascular proliferation and extraction fraction (E) (Table 2), we found that blood flow (Fb) and extraction fraction (E) were negatively correlated ( $r = -0.34$ ,  $P = 0.02$ ), suggesting that the tumours with low blood flow have more leaky vessels.

The observed reduced blood flow accompanied by increased capillary leakage in tumours with high microvascular proliferation is somewhat puzzling, but may be related to the fact that tumour angiogenesis typically generates vessels that in spite of being numerous, are heterogeneous and coarse making them altogether dysfunctional (Carmeliet and Jain, 2011). The reduced flow is considered to be due to the increased leakiness of tumour vessels, also suggested in our data, through which escaping fluid raises the interstitial fluid pressure (Carmeliet and Jain, 2011). The notion of dysfunctional tumour vessels is also supported by the observed tendency of positive correlation between microvascular proliferation and capillary transit time (Tc) (Table 2), which is considered a marker of vessel heterogeneity. Similarly, for rectal cancer a negative correlation has been observed between MVD (using CD31 staining) and transfer from the blood to EES (Ktrans) at DCE-MRI (Atkin *et al*, 2006), suggesting that similar physiological mechanisms related to dysfunctional tumour microvasculature may exist for other tumour types as well.

This study confirms previous findings of a significant prognostic impact of the histological biomarker reflecting microvascular proliferation (Stefansson *et al*, 2006). The negative correlation to blood flow (Fb) accompanied by the negative prognostic impact of low tumour blood flow (Fb) suggests that tumour hypoxia may have a pivotal role in the pathogenic mechanisms leading to tumour growth and metastatic spread in endometrial cancer. Tumour hypoxia is described as a characteristic feature of various solid tumours and is believed to promote tumour progression, resistance to therapy and transformation to more aggressive phenotypes (Vaupel and Mayer, 2007; Carmeliet and Jain, 2011). Preclinical models of cervical cancer and melanoma xenografts have shown that the highly metastatic tumours have a greater

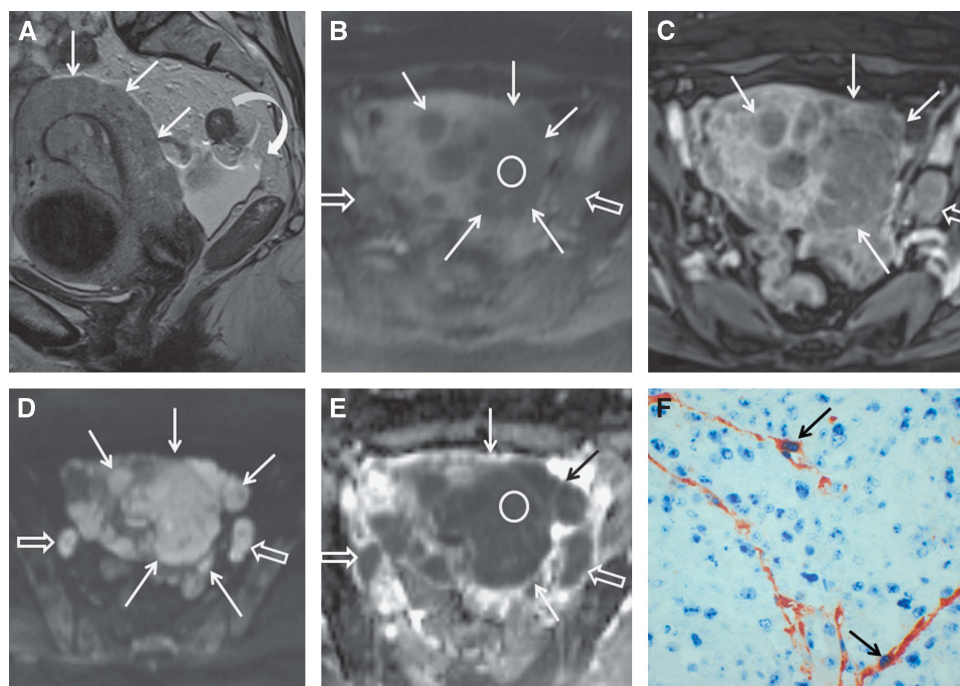


**Figure 3.** Sagittal (A) and axial (B–E) T2-weighted image (A), DCE image (B) with encircled ROI for calculation of DCE-MRI parameters, contrast-enhanced T1-weighted image (C), B1000 (D) and ADC map (E) of the uterus and immunohistochemical staining of tumour tissue (F) in a 66-year-old postmenopausal female with an undifferentiated carcinoma (FIGO stage 3C2). The large uterine tumour invading  $\geq 50\%$  of the myometrial wall is inhomogeneous and hyperintense (closed arrows) on T2-weighted image (A) and hypointense (closed arrows) relative to the normal myometrial tissue on DCE image (B) and contrast-enhanced T1-weighted image (C). Calculated tumour blood flow (Fb) in the encircled ROI (B) was 3.5 ml/100 ml per minute indicating low blood flow. B1000 (D) depicts hyperintense tumour tissue (arrows) and corresponding hypointensity on ADC map (E) indicating restricted diffusion with a mean ADC value of  $0.60 \times 10^{-3} \text{ mm}^2 \text{ s}^{-1}$  within the encircled ROI (E). Enlarged metastatic pelvic lymph nodes (B–F; open arrows) and peritoneal fluid in the recto-uterine pouch (A, curved arrow) were identified preoperatively. Immunohistochemical staining with Ki76/factor VIII (F; magnification  $\times 400$ ; arrows depict proliferating cells) showed 21 proliferating vessels per  $\text{mm}^2$  indicating high microvascular proliferation in the tumour. The patient was diagnosed with liver and lung metastases 5 months after primary surgical treatment (simple hysterectomy and bilateral oophorectomy) while still receiving adjuvant chemotherapy (carboplatin/paclitaxel).

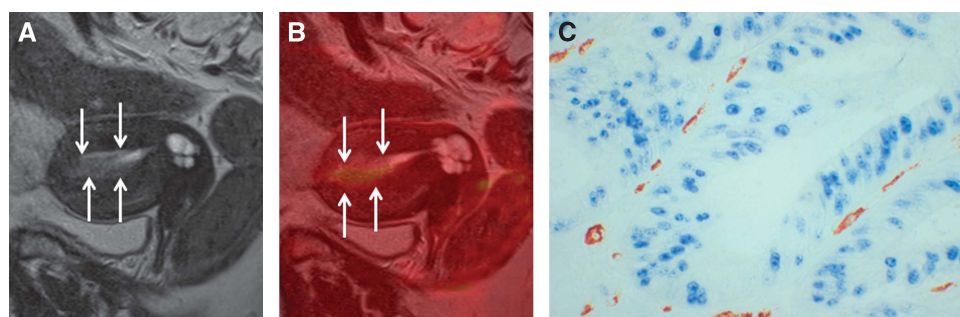


**Figure 4.** Sagittal T2-weighted image (A), fused B1000 and T2-weighted image (B) and immunohistochemical staining of tumour tissue (C) in a 41-year-old premenopausal female with an endometrioid carcinoma (FIGO stage 1A). The tumour (arrows) invades  $< 50\%$  of the myometrial wall and is hyperintense on T2-weighted image and exhibits restricted diffusion with a mean ADC value of  $0.93 \times 10^{-3} \text{ mm}^2 \text{ s}^{-1}$ . Calculated tumour blood flow (Fb) was 13.5 ml per 100 ml per minute indicating relatively high blood flow. Immunohistochemical staining with Ki76/factor VIII (C; magnification  $\times 400$ ) showed low microvascular proliferation (0 proliferating vessels per  $\text{mm}^2$ ). The patient received primary treatment with hysterectomy and bilateral oophorectomy and had no signs of recurrence/progression during the following 3 years.

fraction of hypoxic tissue using pimonidazole as hypoxia marker (Ovrebo *et al*, 2012) and lower values for transfer from the blood to EES (Ktrans) based on DCE-MRI (Ovrebo *et al*, 2012, 2013), both supporting hypoxia-associated metastatic spread in these cancer subtypes. An immunohistochemical study of endometrial carcinomas also reported increasingly expressed hypoxia inducible factor-1 $\alpha$  (HIF-1 $\alpha$ ) from early stages through advanced stages (Ozбудak *et al*, 2008), supporting the importance of hypoxia for tumour progression in endometrial carcinomas.

Interestingly, as opposed to the significant correlations observed for microvascular proliferation and DCE-MRI parameters, no correlations were identified for MVD and the DCE-MRI parameters (Table 2). Thus, we infer that MVD to a lesser extent reflects the pathophysiology of the angiogenic microvessels than the amount of proliferating microvessels. Similarly, for breast cancer the proliferating microvessels reportedly express ongoing angiogenesis and predicts patient outcome better than the more commonly used tissue marker MVD (Arnes *et al*, 2012).

The observed lack of correlation between tumour ADC value and microvascular proliferation or MVD (Table 2) suggests that the tissue-based angiogenic profile of the tumour is only moderately related to changes in cellular density and extracellular space, being reflected in the tumour ADC value (Tamai *et al*, 2007). In line with this, no prognostic value of the preoperative tumour ADC value in endometrial carcinomas was previously reported (Haldorsen *et al*, 2013). Still, the relatively low number of patients studied calls for caution in the conclusion regarding negative findings.

This study has some limitations. First, exact colocalisation between histological sections and DCE-MRI tumour planes for ROI analyses was not possible, implying that the tumour tissue examined for microvascular proliferation is not necessarily included in the tumour volume, in which the functional characteristics of the vasculature are assessed. However, the ROI was placed in an apparently representative part of the tumour and reflects the 'average' functional characteristics of the tumour vasculature in a relatively large tumour volume potentially being more representative of the vascular profile of the entire tumour. Second, for calculation of the perfusion and diffusion parameters, the ROI analysis did not incorporate any spatial information as opposed to a voxel-by-voxel analysis that could potentially have detected microvascular heterogeneity. Furthermore, histogram analyses of the ROIs could potentially have provided additional information regarding the extent of tumour heterogeneity, which has been shown to yield prognostic information in various other malignant tumours (Davnall *et al*, 2012). The current approach was, however, chosen due to the higher signal-to-noise ratio ensuring more reliable quantitative parameter estimations. Third, the analysed ROIs did not comprise the entire tumour volume, as the ROIs were drawn on a single slice and the periphery of the tumour as well as necrotic areas were intentionally excluded from the ROIs. This was, however, done in order to limit the inclusion of the necrotic tissue or normal myometrial tissue (that would otherwise be included due to minimal temporal changes in uterine position due to arterial pulsation and bowel peristalsis) in the analysed ROIs.

In summary, endometrial carcinomas that exhibit increased microvascular proliferation have lower tumour blood flow (Fb) *in vivo* assessed by DCE-MRI. Both microvascular proliferation and tumour blood flow have a significant impact on recurrence/progression-free survival in endometrial carcinomas. Our findings are consistent with the hypothesis that disorganised angiogenesis with coexisting vascular proliferation and hypoxia promotes tumour progression and metastatic spread in endometrial carcinomas. Dynamic contrast-enhanced magnetic resonance imaging may offer a potential for early prediction of angiogenesis-related resistance to treatment (Wilson and Hay, 2011) or response to drugs targeting angiogenesis, but further studies in patients undergoing such treatment are needed to assess the clinical applicability.

## ACKNOWLEDGEMENTS

This study was supported by The Western Norway Regional Health Authority, Research Funds at the Department of Radiology, Haukeland University Hospital, MedViz, Norwegian Research Council, The University of Bergen, The Meltzer Foundation, and The Norwegian Cancer Society (The Harald Andersen's legacy).

## CONFLICT OF INTEREST

The authors declare no conflict of interest.

## AUTHOR CONTRIBUTIONS

ISH, IS, RG, LAA and HBS conceived and designed the study. IS and LAA served as certified pathologist and were responsible for the immunohistochemical data. ISH, RG, JAH, IJM and TT were responsible for the reading of the diagnostic MRIs and for post-processing of the DCE-MRI. HMJW, LB, JT and HBS were responsible for collection of clinical patient data. ØOS provided statistical advice regarding the applied statistical tests. ISH wrote the paper. All authors read and approved the final manuscript.

## REFERENCES

- Amant F, Moerman P, Neven P, Timmerman D, Van LE, Vergote I (2005) Endometrial cancer. *Lancet* **366**(9484): 491–505.
- Arnes JB, Stefansson IM, Straume O, Baak JP, Lonning PE, Foulkes WD, Akslen LA (2012) Vascular proliferation is a prognostic factor in breast cancer. *Breast Cancer Res Treat* **133**(2): 501–510.
- Atkin G, Taylor NJ, Daley FM, Stirling JJ, Richman P, Glynne-Jones R, d'Arcy JA, Collins DJ, Padhani AR (2006) Dynamic contrast-enhanced magnetic resonance imaging is a poor measure of rectal cancer angiogenesis. *Br J Surg* **93**(8): 992–1000.
- Baluk P, Morikawa S, Haskell A, Mancuso M, McDonald DM (2003) Abnormalities of basement membrane on blood vessels and endothelial sprouts in tumors. *Am J Pathol* **163**(5): 1801–1815.
- Carmeliet P, Jain RK (2011) Molecular mechanisms and clinical applications of angiogenesis. *Nature* **473**(7347): 298–307.
- Davnall F, Yip CS, Ljungqvist G, Selmi M, Ng F, Sanghera B, Ganeshan B, Miles KA, Cook GJ, Goh V (2012) Assessment of tumor heterogeneity: an emerging imaging tool for clinical practice? *Insights Imaging* **3**(6): 573–589.
- Fox SB, Gasparini G, Harris AL (2001) Angiogenesis: pathological, prognostic, and growth-factor pathways and their link to trial design and anticancer drugs. *Lancet Oncol* **2**(5): 278–289.
- Gruner R, Taxt T (2006) Iterative blind deconvolution in magnetic resonance brain perfusion imaging. *Magn Reson Med* **55**(4): 805–815.
- Haldorsen IS, Gruner R, Husby JA, Magnussen JJ, Werner HM, Salvesen OO, Bjorge L, Stefansson I, Akslen LA, Trovik J, Taxt T, Salvesen HB (2013) Dynamic contrast-enhanced MRI in endometrial carcinoma identifies patients at increased risk of recurrence. *Eur Radiol* **23**(10): 2916–2925.
- Haldorsen IS, Husby JA, Werner HM, Magnussen JJ, Rorvik J, Helland H, Trovik J, Salvesen OO, Espeland A, Salvesen HB (2012) Standard 1.5-T MRI of endometrial carcinomas: modest agreement between radiologists. *Eur Radiol* **22**(7): 1601–1611.
- Haldorsen IS, Salvesen HB (2012) Staging of endometrial carcinomas with MRI using traditional and novel MRI techniques. *Clin Radiol* **67**(1): 2–12.
- Kinkel K, Forstner R, Danza FM, Oleaga L, Cunha TM, Bergman A, Barentsz JO, Balleyguier C, Brkljacic B, Spencer JA (2009) Staging of endometrial cancer with MRI: Guidelines of the European Society of Urogenital Imaging. *Eur Radiol* **19**(7): 1565–1574.
- Leach MO, Morgan B, Tofts PS, Buckley DL, Huang W, Horsfield MA, Chenevert TL, Collins DJ, Jackson A, Lomas D, Whitcher B, Clarke L, Plummer R, Judson I, Jones R, Alonzi R, Brunner T, Koh DM, Murphy P, Waterton JC, Parker G, Graves MJ, Scheenen TW, Redpath TW, Orton M, Karczmar G, Huisman H, Barentsz J, Padhani A (2012) Imaging vascular function for early stage clinical trials using dynamic contrast-enhanced magnetic resonance imaging. *Eur Radiol* **22**(7): 1451–1464.
- Øvrebo KM, Ellingsen C, Galappathi K, Rofstad EK (2012) Dynamic contrast-enhanced magnetic resonance imaging of the metastatic potential of melanoma xenografts. *Int J Radiat Oncol Biol Phys* **83**(1): e121–e127.
- Øvrebo KM, Ellingsen C, Hompland T, Rofstad EK (2013) Dynamic contrast-enhanced magnetic resonance imaging of the metastatic potential of tumors: a preclinical study of cervical carcinoma and melanoma xenografts. *Acta Oncol* **52**(3): 604–611.
- Ozbudak IH, Karaveli S, Simsek T, Erdogan G, Pestereli E (2008) Neoangiogenesis and expression of hypoxia-inducible factor 1 $\alpha$ , vascular endothelial growth factor, and glucose transporter-1 in endometrioid type endometrium adenocarcinomas. *Gynecol Oncol* **108**(3): 603–608.

- Padhani AR, Liu G, Koh DM, Chenevert TL, Thoeny HC, Takahara T, Dzik-Jurasz A, Ross BD, Van CM, Collins D, Hammoud DA, Rustin GJ, Taouli B, Choyke PL (2009) Diffusion-weighted magnetic resonance imaging as a cancer biomarker: consensus and recommendations. *Neoplasia* **11**(2): 102–125.
- Pecorelli S (2009) Revised FIGO staging for carcinoma of the vulva, cervix, and endometrium. *Int J Gynaecol Obstet* **105**(2): 103–104.
- Salvesen HB, Haldorsen IS, Trovik J (2012) Markers for individualised therapy in endometrial carcinoma. *Lancet Oncol* **13**(8): e353–e361.
- Silverberg SG, Kurman RJ, Nogales F (2003) Tumors of the uterine corpus. In *Tumours of the Breast and Female Genital Organs. World Health Organization Classification of Tumours. Pathology & Genetics*, Tavassoli FA, Devilee P (eds), pp 217–258. IACR Press Inc.: Lyon, France.
- St Lawrence KS, Lee TY (1998) An adiabatic approximation to the tissue homogeneity model for water exchange in the brain: I. Theoretical derivation. *J Cereb Blood Flow Metab* **18**(12): 1365–1377.
- Stefansson IM, Salvesen HB, Akslen LA (2006) Vascular proliferation is important for clinical progress of endometrial cancer. *Cancer Res* **66**(6): 3303–3309.
- Tamai K, Koyama T, Saga T, Umeoka S, Mikami Y, Fujii S, Togashi K (2007) Diffusion-weighted MR imaging of uterine endometrial cancer. *J Magn Reson Imaging* **26**(3): 682–687.
- Taxt T, Jirik R, Rygh CB, Gruner R, Bartos M, Andersen E, Curry FR, Reed RK (2012) Single-channel blind estimation of arterial input function and tissue impulse response in DCE-MRI. *IEEE Trans Biomed Eng* **59**(4): 1012–1021.
- Tofts PS, Brix G, Buckley DL, Evelhoch JL, Henderson E, Knopp MV, Larsson HB, Lee TY, Mayr NA, Parker GJ, Port RE, Taylor J, Weisskoff RM (1999) Estimating kinetic parameters from dynamic contrast-enhanced T(1)-weighted MRI of a diffusable tracer: standardized quantities and symbols. *J Magn Reson Imaging* **10**(3): 223–232.
- Vaupel P, Mayer A (2007) Hypoxia in cancer: significance and impact on clinical outcome. *Cancer Metastasis Rev* **26**(2): 225–239.
- Weidner N, Semple JP, Welch WR, Folkman J (1991) Tumor angiogenesis and metastasis—correlation in invasive breast carcinoma. *N Engl J Med* **324**(1): 1–8.
- Wilson WR, Hay MP (2011) Targeting hypoxia in cancer therapy. *Nat Rev Cancer* **11**(6): 393–410.

This work is published under the standard license to publish agreement. After 12 months the work will become freely available and the license terms will switch to a Creative Commons Attribution-NonCommercial-Share Alike 3.0 Unported License.